International Journal of Mechanical, Industrial and Aerospace Sciences
ISSN: 2517-9950
Vol:7, No:6, 2013

Spreading of Swirling Double–Concentric Jets at Low and High Pulsation Intensities

Shiferaw R. Jufar, Rong F. Huang, and Ching M. Hsu

***Abstract*—**The spreading characteristics of acoustically excited swirling double-concentric jets were studied experimentally. The central jet was acoustically excited at low and high pulsation intensities. A smoke wire flow visualization and a hot-wire anemometer velocity measurement results show that excitation forces a vortex ring to roll-up from the edge of the central tube during each excitation period. At low pulsation intensities, the vortex ring evolves downstream, and eventually breaks up into turbulent eddies. At high pulsation intensities, the primary vortex ring evolves and a series of trailing vortex rings form during the same period of excitation. The trailing vortex rings accelerate while evolving downstream and overtake the primary vortex ring within the same cycle. In the process, the primary vortex ring becomes unstable and breaks up early. The effect of the fast traveling trailing vortex rings combined with the swirl motion of the annular flow improve jet spreading compared with the naturally evolving jets.

***Keywords*—**Acoustic excitation, double–concentric jets, flow control, swirling jet.

I. Introduction

SWIRLING jets have been used in many practical applications. Particularly for combustion applications, swirling jets provide better flame stabilization by forming a recirculation zone. The swirl number required to create the recirculation zone is rather high, about 0.6 [1]. In an effort to establish the recirculation zone at lower swirl number, [2] studied swirling jet by placing a central blockage disk at the exit of the test section. They found that at a blockage ratio higher that 0.1, the swirl number required to form the recirculation zone can be lowered significantly. In another study [3], they investigated flow structure and turbulence properties of swirling double-concentric jets in which a central jet is injected into a swirling wake. Although the recirculation zone can be formed at lower swirl numbers, strong mixing was not achieved due to the injection-through problem. The central jet directly flushes downstream without much interaction with the swirling recirculation wake.

Huang and Yen [4] developed a passive flow control method to circumvent the injection-through problem by placing a small circular disk at some distance downstream the blockage disk. They showed that such arrangement creates significant increase in turbulence fluctuations and momentum exchange which improve mixing considerably compared with the flow without the control disk. Several other investigators studied active flow control methods like jet excitation to enhance the mixing and combustion processes [5]–[7].

The sensitivity of a jet to an external excitation has been known for several decades. Excitation either enhances or suppresses jet mixing rate, noise generation and turbulent properties [8], [9]. Under certain conditions, jet excitation improves mixing during the growth of large-scale coherent structures and their subsequent breakdown into small-scale turbulence. Entrainment and mixing properties of excited swirling and non swirling single jets were investigated by many authors [10]–[12]. Huang et al. [13] studied swirling double-concentric jets subject to acoustic excitation. They identified several flow modes based on the excitation Strouhal number and pulsation intensity. It was shown that higher frequency excitation saturate near the central tube exit while the effect of lower frequency continues further downstream. The turbulence properties and dispersion characteristics of each flow mode was discussed. The mixing was drastically improved when compared with unexcited flow.

In this study, as an extension of the previous work [13], jet spreading at low Strouhal number excited with low and high pulsation intensity was investigated. The excitation Strouhal number was fixed while two pulsation intensities, one low and the other high, were considered. Smoke-wire flow visualization was used to render the flow field. Hot-wire anemometer velocity measurement technique was used to measure the velocity instabilities. The results were compared and the mechanisms of the jet spreading were discussed.

II. Experimental Methods

A. Experimental Setup

Fig. 1 shows the apparatus used in the present study. The annular flow was supplied from a ring blower. The air was passed through an acoustic filter to suppress ripples from the rotation of the bower blades. A pressure regulator and a calibrated rotameters were installed to regulate the flow rate before it enters the plenum chamber. The flow then passed through a honeycomb, mesh screen, and a settling chamber to reduce turbulence fluctuations. To impart swirl to the annular flow, 12 guide vanes were installed in a pitch circle with a radius 175mm. A nozzle with a contraction ratio of 9.0 was

S. R. Jufar is with the Department of Mechanical Engineering, National Taiwan University of Science and Technology, Taipei 10607, Taiwan, ROC (phone: 886-2-2737-6488; fax: 886-2-2737-6460; e-mail: d9903802@mail.ntust.edu.tw).

R. F. Huang is with the Department of Mechanical Engineering, National Taiwan University of Science and Technology, Taipei 10607, Taiwan, ROC (e-mail: rfhuang@mail.ntust.edu.tw).

C. M. Hsu is with the Graduate Institute of Applied Science and Technology, National Taiwan University of Science and Technology, Taipei 10607, Taiwan, ROC (e-mail: cmhsu@mail.ntust.edu.tw).

used to accelerate the flow. A cylindrical pipe with inside diameter D_o = 40mm was attached at the exit of the nozzle. A circular stainless-steel disk with a thickness of 1mm and a diameter D = 30mm was placed in the annulus to serve as a bluff body. A 5mm diameter hole was made at the center of the disk to vent the central jet into the swirling wake. A cylindrical coordinate, axial (x) and radial (r), was defined to originate from the horizontal plane at the center of the blockage disk. The annular flow Reynolds number based on hydraulic diameter of the annulus and the annular volumetric mean axial velocity was 144. The corresponding swirl number, defined as a ratio of the axial flux of angular momentum to the axial flux of axial momentum [1], was 0.126.

The central jet was supplied from an air compressor. The jet went through a pressure regulator and a calibrated rotameter. Then, it was connected to the plenum of a nozzle with a contraction ratio of 900 and length 300mm. At the exit of the nozzle, a stainless-steel tube of length L_t = 600mm, an external diameter of 6.4mm, and an internal diameter of d = 5mm was connected. The other end of the tube was connected to the hole made at the center of the blockage disk to inject the central jet into the swirling wake. The Reynolds number of the central jet based on the tube diameter d and the central jet volumetric mean axial velocity u_c was 500. The central jet was excited by a loudspeaker placed inside the plenum of the nozzle. The face diameter of the loudspeaker was 300mm. The voice coil resistance measured across its terminals was 6.6 Ω. A square waveform from a function generator, verified by an oscilloscope, was modulated by a power amplifier to drive the loudspeaker at 20 Hz.

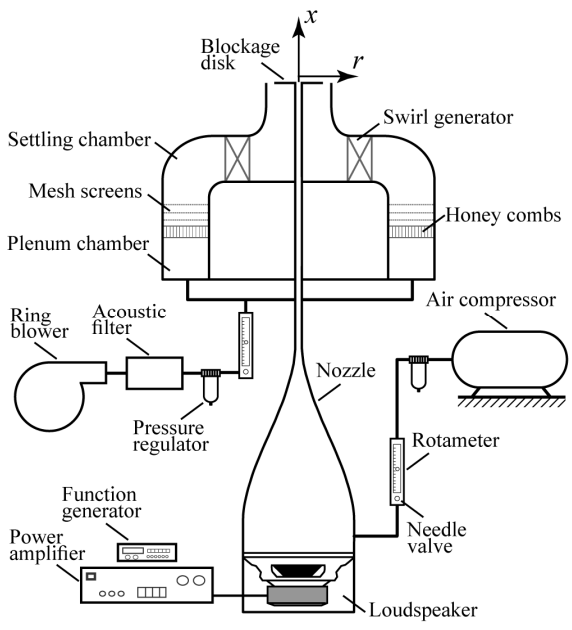

Fig. 1 Experimental setup

B. Flow Visualization

A smoke-wire flow visualization technique was used to reveal the flow streaklines. A corrugated tungsten wire with a diameter of 200μm was place in the symmetric plane across the jet exit at x = 1mm. The wire terminals were connected to a voltage source to generate a smoke by heating mineral oil brush-coated on the wire. The long exposure images were captured by passing the central air through a smoke generator where it entrained a kerosene oil mist. A dual head Nd:YLF laser beam, made into a 0.5mm thick laser sheet by a set of optics, was used as a light source to illuminate the flow field. The wave length and maximum pulse rate were 527nm and 10, 000 pulses/s, respectively. An IDT X-stream XS-4 high-speed camera was used to capture the instantaneous flow images. The spatial resolution of the instantaneous images was 0.153mm/pixle. The exposure time and the frame rate of the instantaneous images were 300μs and 3000 Hz, respectively. A canon EOS 450D still camera was used to recorded the long exposure images. The spatial resolution of the long-exposure images was 0.055mm/pixle. The exposure time was 3s. The jet spread width W was estimated from the long exposure images. The radial locations where the gray-level values change abruptly from zero to greater than zero were considered as jet boundaries.

C. Velocity Measurement

A one-component hot-wire anemometer was used to measure the velocity instabilities. The hot-wire probe used was TSI 1210-T1.5. The probe was attached to an arm of a three-dimensional traversing mechanism to move it between the measuring positions. The hot-wire anemometer was calibrated in a wind tunnel using a pitot tube associated with a high-precision electronic pressure transducer. The hot-wire signal was passed through a low-pass filter set at 6 kHz. A high-speed data acquisition system was used to record the signals at 20, 000 samples/s for 3s.

III. Results and Discussion

A. Jet Pulsation

The velocity pulsation at the exit of the central tube was recorded with a one-component hot-wire anemometer positioned at the center of the blockage disk at x/D = 0.067. A 20 Hz square waveform from the function generator was modulated by the power amplifier to drive the loudspeaker. The signals from the Hot-wire probe, the function generator, and the power amplifier were recorded at the same time. There was no phase lag between the signals from the function generator and the power amplifier. However, the signal from the power amplified was inverted due to the arrangement of the circuitry. The phase angle α = 0, used to describe the flow evolution process, was set to begin from the rising edge of the power amplifier signal. The rising edge of the velocity signal presented a phase lag of about 20% behind the power amplifier. To quantify the intensity of forcing, pulsation intensity was defined as u'_{c0}/u_c. It is a ratio between root-mean-square velocity and volumetric mean axial velocity. The

Strouhal number defined as $St_{exc} = f_{exc} d / u_c$ was 0.06. Here, f_{exc} is the excitation frequency.

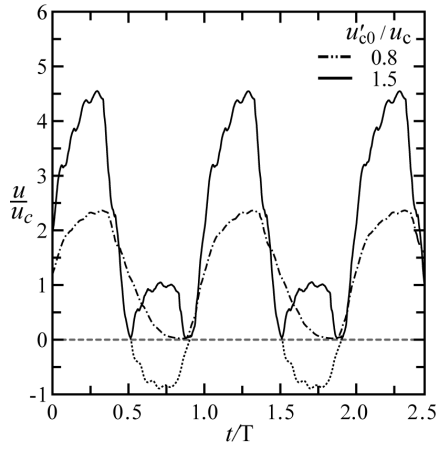

Fig. 2 Time history of velocity measured at $x/D = 0.067$, $r/D = 0$

Fig. 2 shows velocity histories at two pulsation intensities. The velocity profile presents a periodic oscillation with the same period as the excitation signal. Clearly, the amplitude of the velocity at the pulsation intensity 1.5 is much larger than that of 0.8. At higher pulsation intensity, higher than 1.0, the velocity at the exit becomes negative for a significant portion of the excitation period. The dashed curves, indicating the negative velocity, were a reconstitution of the mirror image of the small humps above the zero velocity line shown in gray color. This happens due to the directional indistinctness of the hot-wire probe which records only positive values. However, this phenomenon was verified from movies recorded during flow visualization which shows the jet was being sucked back into the central tube during the same periods as the small humps appear in the velocity time history.

There are several types of actuators to excite a jet. A piston/cylinder arrangement has been used by several investigators to study vortex ring dynamics. In such case, the forcing intensity is usually defined as a stroke ratio *L/D*. It is a ratio between length of a column of fluid and exit diameter of a nozzle. Gharib et al. [14] used a piston/cylinder device to study vortex ring formation in a starting jet. In general, increasing a stoke ratio would increase the circulation of a vortex ring. They showed that a universal time scale about 4 is a limiting condition that further increase in stoke ratio does not increase the circulation, and Hence the growth of the vortex ring. In the present study, an attempt was made to calculate the equivalent stroke ratio to the pulsation intensity used. The length of the fluid column can be calculated by integrating the velocity profile over a half period during which time the velocity stays higher than the mean value. However, the study of Aydemir et al. [15] showed that for sinusoidal forcing, the integration limits that determines the circulation of the vortex ring are actually from 0 to 1/3*T*, where *T* is period of excitation. Hence, the equivalent stroke ratio at pulsation intensities 0.8 and 1.5 was about 3.4 and 6.0 respectively.

B. Flow Evolution

Fig. 3 shows the flow evolution process of the swirling double-concentric jets excited at 20 Hz. The Strouhal number at this excitation frequency was 0.06. The dashed gray line separates excitation at the pulsation intensities 0.8 and 1.5. But other flow conditions remain the same. In both cases a single vortex ring visually appear at the exit of the central tube around α = 50°. At the pulsation intensity 0.8, as shown in Fig. 3 (a)-(d), the vortex ring #1 evolves downstream and eventually become less coherent and breaks up into turbulent eddies.

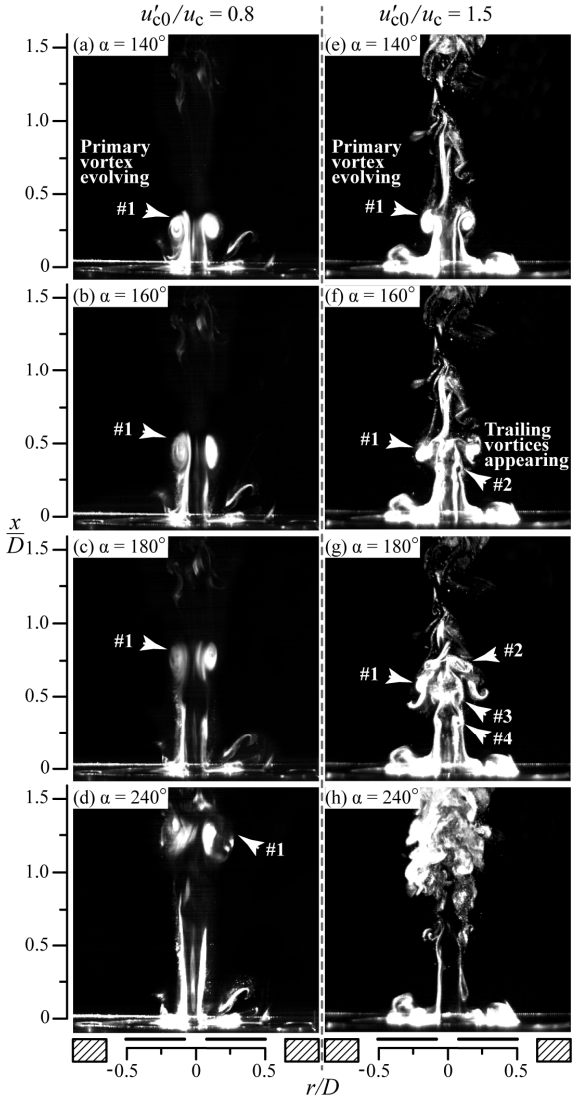

Fig. 3 Flow evolution process

At the pulsation intensity 1.5, a primary vortex ring #1 appears similar to the lower pulsation intensity and continues to evolve downstream as shown in Fig. 3 (e). Around the phase

angle α = 160°, a trailing vortex ring #2 appears as shown in Fig. 3 (f). Subsequently, several other trailing vortex rings like #3 and #4 form. These vortex rings accelerate downstream to overcome the primary vortex ring marked #1 as shown in Fig. 3 (g). The primary vortex ring becomes unstable and breaks up earlier as the trailing vortex rings pass through it. The jet diameter and the recirculation bubble size reduce periodically due to the suction back effect of higher pulsation intensity shown in Fig. 2. As the vortex rings evolve downstream, they also rotate about the central axis due to the swirling motion of the annular flow. At higher pulsation intensities, the combined effect of the trailing vortex rings and swirling motion of the annular flow enhance the central jet spreading significantly as shown in Fig. 3 (h).

As discussed previously, the equivalent stroke ratio at the pulsation intensity 0.8 was about 3.4. At this forcing strength, the vortex ring was not saturated and it was able to entrain more circulation. At the pulsation intensity 1.5, the equivalent stroke ratio was about 6.0. Such large stroke ratio generates more circulation than the primary vortex can entrain. Hence, the excess circulation forms a series of trailing vortex rings in the wake of the primary vortex ring similar to the observations made by [14], [15].

However, in the present study the jet was not flowing into a quiescent environment like the studies of starting jet discussed earlier in which a limiting stroke ratio which is a time scale about 4 exists. The effect of background co-flow was studied in the work of Krueger et al. [16]. They observed that the value of the limiting stroke ratio drops with the presence of uniform background flow. The observations from the present study, where an acoustically excited central jet is injected into a weakly swirling wake, appear to conform to the results of the starting jets and no significant drop in formation number was observed. Apparently, effect of stronger swirl numbers should be significant and need to be investigated in detail for better understanding.

C. Jet Spreading

Fig. 4 shows the long-exposure images of the swirling double concentric jets excited at pulsation intensity 0.8, Fig. 4 (a), and 1.5, Fig. 4 (b). To visualize the spreading characteristics of the central jet, smoke was released only through the central jet. Hence, the swirling wake is not visible. At pulsation intensity 0.8, the jet diameter remains almost constant upstream x/D = 1.5. Downstream this point, the vortex rings start to become less coherent and break up into turbulent eddies and the jet starts to expand significantly. Using the abrupt gray-level change, the jet width expansion W/D at x/D = 2.5 is about 0.96. At pulsation intensity 1.5, the jet diameter remains almost the same until about x/D = 0.7. However, it is slightly narrower than the jet at pulsation intensity 0.8. This might be attributed to the suction back effect which stretches the jet and chocks the central flow periodically. Downstream x/D = 0.7, the central jet starts to expand considerably. At x/D = 2.5, W/D = 1.26. At his level, the jet spreading was increased by about 30% compared to the pulsation intensity 0.8. The improvement in spreading width is attributed to the effect of the fast travelling trailing vortex rings shown in Fig. 3 (g). As these vortex rings accelerate downstream and pass through the primary vortex ring, they make it unstable and urge the primary vortex to break up earlier. Although the central jet at high pulsation intensity starts to spread earlier, it seems that the spread angle does not change significantly compared with the low pulsation intensity excitation. However, further investigations are required to study the effect of larger pulsation intensities on the jet spreading angle.

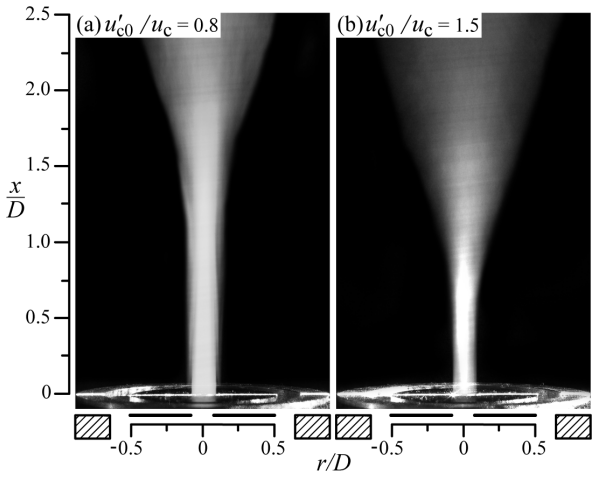

Fig. 4 Long-exposure images

D. Velocity Characteristics

Fig. 5 shows the velocity history and power spectrum density function on the centerline at x/D = 1.5. The velocity profile at the pulsation intensity 0.8, shown in Fig. 5 (a), presents a periodic fluctuation with a peak value about 2m/s. As can be seen from the flow evolution pictures, Fig. 2 (d), the vortex ring at this level appears coherent. Hence, the velocity profile shows no significant fluctuating velocity components. The corresponding power spectrum density function shown in Fig. 5 (b) indicates a peak at 20 Hz. This is the same as the excitation waveform frequency. Evidently, the vortex rings are evolving with the same frequency as the excitation signal. Counting the number of vortex rings evolving from the flow visualization images also shows that the vortex rings are evolving at the same frequency as the excitation signal.

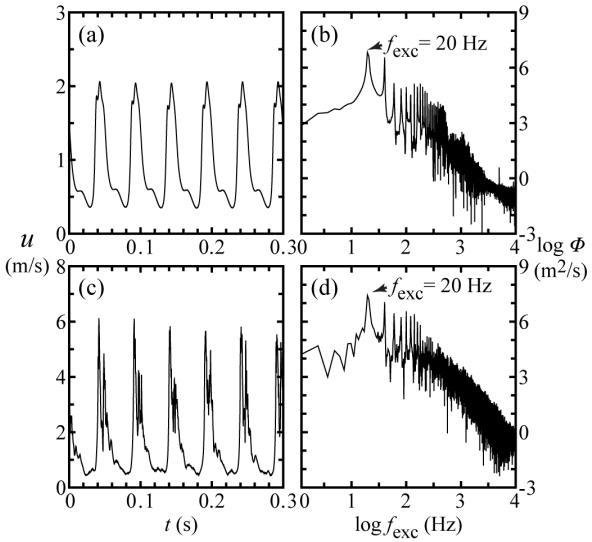

Fig. 5 Velocity history and power spectrum density

Fig. 5 (c) shows the velocity history at x/D = 1.5 when the flow was excited at the pulsation intensity 1.5. The velocity profile shows turbulence superimposed periodic fluctuations when compared to the profile at the pulsation intensity 0.8. Fig. 5 (d) shows the corresponding power spectrum density. It shows a dominant frequency peak at 20 Hz which is the same as the excitation frequency. This indicates that at this level, the primary vortex ring did not fully break up and a trace of the coherent vortex ring was still present.

Fig. 6 shows the fluctuation intensities along the centerline of the swirling double-concentric jets. At the pulsation intensity 0.8, the velocity fluctuation gradually decreases along the centerline until about x/D = 1.3. Downstream x/D = 1.3, the fluctuation intensity decreases quickly which is an indication that the jet spreading was enhanced. The long exposure flow visualization image, Fig. 4 (a), supports the result observed from the velocity fluctuation measurements. It shows significant increase in spreading start about the same level as the fluctuation intensity gradient changes. At the pulsation intensity 1.5, the velocity fluctuation decreases linearly along the centerline but at steeper gradient compared to the case at the pulsation intensity 0.8. The fluctuation intensity decays faster downstream about x/D = 1.0. Similarity, the jet spreading was enhanced significantly starting from this level as shown in Fig. 4 (b).

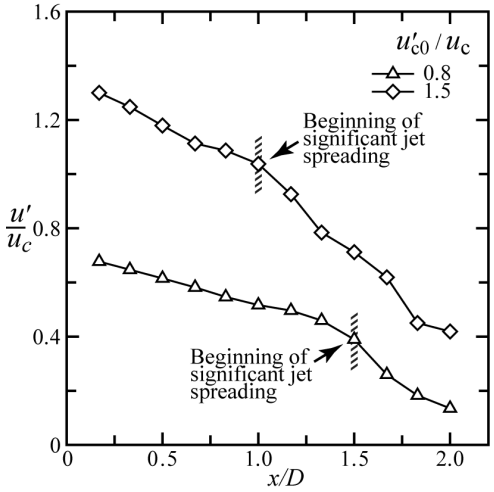

Fig. 6 Fluctuation intensity variation along the centerline

IV. Conclusions

Flow behaviors and jet spreading characteristics between low and high pulsation intensity excitation of the swirling double–concentric jets were compared. In both cases, a single vortex ring evolves from the edge of the central tube with the same period as the excitation signal. At low pulsation intensity, the vortex ring continues to move downstream where it eventually becomes less coherent and break up into turbulent eddies. At high pulsation intensities, a number of trailing vortex rings appear behind the leading vortex. These vortex rings quickly accelerate and pass through the primary vortex ring making it to break up earlier. This combined with the swirling motion induced by the recirculation wake spreads the jet faster.

The understanding from the present study could be useful for combustion applications. One can envisage the application of swirling double-concentric jets for industrial burners. Although the jet spreading at higher pulsation intensities is much better than lower pulsation intensities, the suction back effect at larger pulsation intensities may chock the fuel supply for burner applications where combustion happens as a continuous process. However, in pulsed jet engines, where combustion occurs in pulses, the flow behavior shown at high pulsation intensity could be applicable. Although the suction back effect may not be suitable for continues combustion, it could be an advantage in pulsed jet engines as it produces in-tube mixing during the idle cycle of the pulsed combustion. Nevertheless, further investigations are required to fully understand the impacts of the flow behaviors on the combustion process.

References

[1] A. K. Gupta, D. G. Lilley, and N. Syred, "Swirl flows," Abacus, Tunbridge Wells, Kent and Cambridge, Mass, 1984, pp. 13–17.
[2] R.F. Huang, and F.C. Tsai, "Observations of swirling flows behind circular disks," *AIAA Journal*, vol. 39, pp. 1106–1112, 2001.

[3] R.F. Huang, and F.C. Tsai, "Flow field characteristics of swirling double concentric jets, " *Experimental Thermal and Fluid Science*, vol. 25, pp. 151–161, 2001.
[4] R.F. Huang, and S.C. Yen, "Axisymmetric swirling vortical wakes modulated by a control disk," *AIAA Journal*, vol. 41, pp. 888–896, 2003.
[5] S.C. Crow, and F.H. Champagne, "Orderly structure in jet turbulence," *Journal of Fluid Mechanics*, vol. 48, pp. 547–591, 1971.
[6] S.K. Oh, and H.D. Shin, "A visualization study on the effect of forcing amplitude on tone-excited isothermal jets and jet diffusion flames," *International Journal of Energy Research*, vol. 22, pp. 343–354, 1998.
[7] K.M. Lee, T.K. Kim, W.J. Kim, S.G. Kim, J. Park, and S. N Keel, "A visual study on flame behavior in tone-excited non-premixed jet flames," *Fuel*, vol. 81, pp. 2249–2255, 2002.
[8] K.B.M.Q. Zaman, and A.K.M.F. Hussain, "Turbulence suppression in free shear flows by controlled excitation, Journal of Fluid Mechanics," vol. 103, pp. 133–159, 1981.
[9] K.B.M.Q. Zaman, and A.K.M.F. Hussain, "Vortex pairing in a circular jet under controlled excitation. Part 1. General jet response," *Journal of Fluid Mechanics*, vol. 101, pp. 449–491, 1980.
[10] S.V. Alekseenko, V.M. Dulin, Y.S. Kozorezov, and D.M. Markovich, "Effect of axisymmetric forcing on the structure of a swirling turbulent jet," *International Journal of Heat and Fluid Flow*, vol. 29, pp. 1699–1715, 2008.
[11] T.K. Kim, J. Park, and H.D. Shin, "Mixing Mechanism near the Nozzle Exit in a Tone Excited Non-Premixed Jet Flame," *Combustion Science and Technology*, vol. 89, pp. 83–100, 1993.
[12] A. Olcay, and P. Krueger, "Measurement of ambient fluid entrainment during laminar vortex ring formation," *Experiments in Fluids*, vol. 44, pp. 235–247, 2008.
[13] R.F. Huang, S.R. Jufar, and C.M. Hsu, "Flow and mixing characteristics of swirling double-concentric jets subject to acoustic excitation," *Experiments in Fluids*, vol. 54, pp. 1–23, 2012.
[14] M. Gharib, E. Rambod, and K. Shariff, "A universal time scale for vortex ring formation," *Journal of Fluid Mechanics*, vol. 360, pp 121–140, 1998.
[15] E. Aydemir, N. Worth, and J. Dawson, "The formation of vortex rings in a strongly forced round jet," *Experiments in Fluids*, vol. 52, pp. 729–742, 2012.
[16] P.S. Krueger, J.O. Dabiri, and M. Gharib, "The formation number of vortex rings formed in uniform background co-flow," *Journal of Fluid Mechanics*, vol. 556, pp. 147-166, 2006.